Calculated magneto-optical Kerr spectra of the half-Heusler compounds AuMnX (X = In, Sn, Sb)



2007 J. Phys.: Condens. Matter 19 315216

(http://iopscience.iop.org/0953-8984/19/31/315216)

IOP PUBLISHING JOURNAL OF PHYSICS: CONDENSED MATTER

J. Phys.: Condens. Matter **19** (2007) 315216 (9pp) doi:10.1088/0953-8984/19/31/315216

# Calculated magneto-optical Kerr spectra of the half-Heusler compounds AuMnX (X = In, Sn, Sb)

**M Amft**[1] **and P M Oppeneer**

Department of Physics, Uppsala University, Box 530, S-751 21 Uppsala, Sweden

E-mail: martin.amft@fysik.uu.se

Received 7 December 2006, in final form 9 February 2007
Published 3 July 2007
Online at stacks.iop.org/JPhysCM/19/315216

**Abstract**

The ferromagnetic ground states of the half-Heusler compounds AuMnX (X = In, Sn, Sb) have been calculated in the framework of the local spin-density approximation (LSDA) to density functional theory (DFT). AuMnSn is computed to be a half-metallic ferromagnet, whereas AuMnIn and AuMnSb are not half-metallic, due to their different band filling. The computed relativistic electronic structures served as inputs to calculate the magneto-optical Kerr rotations and ellipticities for all three materials. In the case of AuMnSn the largest, zero-temperature, polar Kerr rotation has been found to be $-0.45°$ at about 1 eV photon energy. The computed MOKE spectra of AuMnSn are in qualitative agreement with recent experiments. The largest Kerr rotations of AuMnIn and AuMnSb have been calculated to be $+0.64°$ at 4.3 eV and $-0.85°$ at 0.9 eV, respectively.

## 1. Introduction

Ferromagnetic Heusler compounds of the type TMnX (T: d-transition element; X: p-element) which crystallize in the half-Heusler structure $C1_b$ have been studied for several years, since they exhibit a broad spectrum of interesting properties [1–3]. The occurrence of half-metallicity [4, 5] in several Heusler compounds bears promise for applications of these materials in spin-polarized magneto-resistive devices (see, e.g. [6]). One feature of several ternary Heusler compounds is the high spin-moment per unit cell, reaching to, or even above, the maximum predicted by the Slater–Pauling curve [7–9]. Another feature of Heusler compounds which is appealing for applications, is their polar magneto-optical Kerr effect (P-MOKE) [2]. PtMnSb has been of special interest because of its unusually large magneto-optical (MO) Kerr rotation of $-1.27°$ at room temperature [1, 6]. Materials exhibiting large Kerr rotations are being sought, as these are desirable for magneto-optical storage media. Very recently, two relatively new half-Heusler compounds, AuMnSn and AuMnSb, have entered

[1] Author to whom any correspondence should be addressed.

the scientific picture [10, 11]. Polar Kerr rotations as big as $-1^\circ$ were recently predicted by theory for AuMnSn and AuMnSb [12], suggesting the potential of these compounds for magneto-optical recording applications. However, very recently performed measurements of the P-MOKE spectrum of AuMnSn showed a much smaller Kerr rotation of about $-0.22^\circ$ only [13]. The substantial difference between the predicted P-MOKE spectrum and the measured spectrum was attributed [13] to the absence of strong electron correlations in the DFT calculations. While it is in principle possible that additional '$+U$' Coulomb correlations are required, this has previously not found to be the case for Heusler compounds [14, 15]. An exception to this was recently proposed [8].

In the current paper we present the results of our calculations for the electronic ground state and MOKE, i.e. Kerr rotation and ellipticity spectra, of the three compounds AuMnX (X = In, Sn, Sb). The computed ground-state quantities, as magnetic moments and half-metallicity, are in agreement with experimental data and the previous theoretical investigation [11, 12]. Although we applied a computational scheme which gave quantitatively good results for PtMnSb [14, 16], the agreement with experimental data [13] for AuMnSn is qualitative only, but we do not confirm the Kerr rotation of $-1^\circ$ predicted recently [12]. We could, furthermore, show that the quantitative agreement becomes partially better if one artificially reduces the magnetic moments in the material. The Curie temperature is 600 K [10], thus the moments are plausibly reduced in experiments at room temperature.

Along the same lines as for AuMnSn, we calculated also the MOKE spectra of AuMnIn and AuMnSb ($T_c$ = 135 K [18]), although, to our knowledge, only the latter one has been studied in experiments, e.g. [18], and the magneto-optical properties of neither compound have yet been investigated experimentally.

## 2. Methods

### *2.1. Electronic structure calculations*

The *ab initio* electronic structure calculations for the three compounds AuMnX (X = In, Sn, Sb) were performed in the framework of the relativistic density functional theory (DFT) in the local spin density approximation (LSDA). As variational basis functions we used augmented spherical waves (ASW), cf [19], and the spherical potential approximation was applied. An empty atomic sphere has been introduced for the one empty position in the half-Heusler structure, adopting equal or nearly equal radii for all atoms in the unit cell. The applicability of this approach in the case of (half-) Heusler compounds was shown in [16] and [20].

For all band structure calculations self-consistency was obtained with 4352 special $k$-points in the irreducible Brillouin zone (BZ). By calculating the minimal total energy for the ferromagnetic ground state of all three compounds, the respective equilibrium theoretical lattice constants were determined. For AuMnIn a ferromagnetic ground state was assumed because of its structural similarity to the other two compounds.

### *2.2. MOKE calculations*

The intrinsic P-MOKE is approximately described by the equation:

$$\theta_K + i\varepsilon_K \approx \frac{-\sigma_{xy}}{\sigma_{xx}\left(1 + i\frac{4\pi}{\omega}\sigma_{xx}\right)^{1/2}}, \tag{1}$$

cf [21], where $\sigma_{xx}$ and $\sigma_{xy}$ are components of the complex conductivity tensor of the material in question, $\theta_K$ is the angle of the Kerr rotation, $\varepsilon_K$ is the Kerr ellipticity, and $\omega$ the frequency of the incident light.

**Table 1.** Comparison of experimental and calculated results for the AuMnX (X = In, Sn, Sb) series. The experimental values for AuMnSn are taken from [10] and those for AuMnSb from [18]. No experimental data have yet been published for AuMnIn.

| | AuMnIn | AuMnSn | AuMnSb |
|---|---|---|---|
| Exp. $a$ (Å) | — | 6.323 | 6.379 |
| Calc. $a$ (Å) | 6.191 | 6.197 | 6.297 |
| Exp. $\mu_{\mathrm{F}}^{\mathrm{Mn}}$ ($\mu_{\mathrm{B}}$) | — | $3.8 \pm 0.1$ | $4.2 \pm 0.1$ |
| Calc. $\mu_{\mathrm{F}}^{\mathrm{Mn}}$ ($\mu_{\mathrm{B}}$) | 3.79 | 4.01 | 4.24 |

By means of the Kubo linear-response formula [22, 23] the components of the interband conductivity tensor $\tilde{\sigma}$ can be expressed as functions of the computed variables, i.e. the single-particle band energies and matrix elements of momentum operators and a (phenomenological) relaxation time $\tau = \delta^{-1}$, which was treated as state and energy independent in our approach. The crucial point of a MOKE calculation is an accurate evaluation of the matrix elements and the $k$ integration of the irreducible BZ. The latter can be achieved by the so-called analytical tetrahedron technique. An implementation of this *ab initio* scheme, which we applied to compute the necessary components of $\tilde{\sigma}$, has been described in [21].

As an input to the MOKE calculations we used the respective electronic band structure calculated within the ASW framework. In the irreducible BZ 4352 $k$-points were used and it was further divided into 165 888 tetrahedra, on which the numerical integration was performed.

The intraband part of the conductivity can, in a simplified manner, be described by an empirical Drude term,

$$\sigma_{\mathrm{D}} = \frac{\sigma_0}{1 - \mathrm{i}\omega\tau_{\mathrm{D}}}, \tag{2}$$

where the DC Drude conductivity $\sigma_0$ and the Drude relaxation time $\tau_{\mathrm{D}}$ are treated as constants that are often approximately known from experiments. In our MOKE calculations the following input parameters were used: $\sigma_0 = 5 \times 10^{15}\ \mathrm{s}^{-1}$, $\tau_{\mathrm{D}} = 100\ \mathrm{Ryd}^{-1}$. The influence of the Drude term will be shown in section 3. Also, we used a state independent interband relaxation rate $\delta = 0.4$ eV in accordance with [16] and [21]. The impact of adopting different relaxation rates will be shown in the next section, as well.

## 3. Results

### *3.1. Electronic ground state properties*

For all three compounds under consideration, AuMnX (X = In, Sn, Sb), the calculated lattice constants and total magnetic moments for Mn are listed in table 1 together with available experimental data. Taking into account the well known underestimation of the lattice constant by DFT [24] the agreements between theory and experiment are satisfactory. Also the calculated total magnetic moments of Mn agree quite well with the experimental values obtained from extrapolations to 5 K [10, 18]. Even though no data for AuMnIn are available, the calculated lattice constant and total magnetic moment of Mn are physically reasonable.

The spin-projected density of states (DOS) of all three compounds are shown in figure 1. As it can be seen from the gap of the spin-down DOS at the Fermi energy (placed at $E = 0$ eV), the half-Heusler compound AuMnSn is half-metallic. In contrast, the two other compounds, AuMnIn and AuMnSb, are calculated to be ordinary metals due to the one electron less or more, respectively, in the unit cell, and the corresponding band filling.

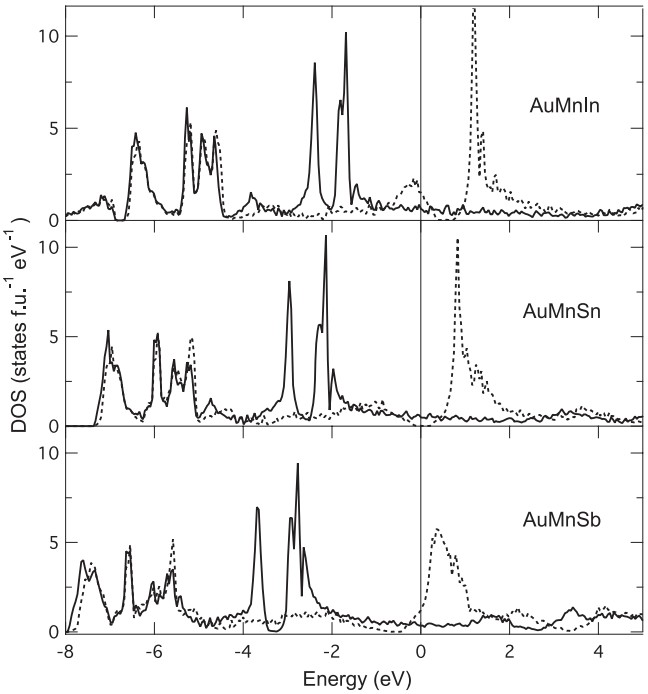


**Figure 1.** Calculated spin-projected DOS for the half-Heusler compounds AuMnIn, AuMnSn and AuMnSb, respectively. Solid lines: spin-up, dashed lines: spin-down. The half-metallicity of AuMnSn can be clearly seen, whereas AuMnIn and AuMnSb are ordinary metals.

### *3.2. MOKE of AuMnSn*

The calculated Kerr rotation $\theta_K$ and ellipticity $\varepsilon_K$ are compared with the experimental outcomes of [13] in figure 2(a). It can be seen that the basic features of the available experimental data, i.e. number and positions of minima and maxima, are reproduced fairly well. However, the overall quantitative agreement could be better. The most striking differences between the calculated and the measured Kerr spectra are, first, the shift of the calculated $\theta_K$ and $\varepsilon_K$ by approximately 0.3 eV towards smaller photon energies and, secondly, the overestimation of the calculated Kerr rotation for photon energies below 2 eV and at 3.1 eV. The largest calculated Kerr rotation of AuMnSn is $-0.45°$ at 0.83 eV. Since the measured $\theta_K$ does not show distinct features above 3.5 eV, which might be due to the used experimental setup, it seems inappropriate to draw any conclusions from the discrepancy between theory and experiment for this energy range.

Obviously the outcome for the Kerr ellipticity is quite similar: all the measured features can in principle be found in the calculated spectrum, but especially for photon energies less than 3.4 eV the size of $\varepsilon_K$ is overestimated by theory. For the small measured peak at 1.5 eV even the sign of $\varepsilon_K$ is not reproduced. As for $\theta_K$ at higher energies, no conclusions concerning the differences in the $\varepsilon_K$ spectra should be drawn for photon energies higher than 4.5 eV.

In figure 2(b) the real and imaginary parts of the (off-) diagonal elements of the optical conductivity tensor $\tilde{\sigma}$, which pertain to the calculated MOKE spectra in figure 2(a), are shown. As can be seen in the upper panel, the spectrum of the diagonal element $\sigma_{xx}$ is rather structureless. Yet, some features of the Kerr rotation spectrum can be related to it. For instance, the side peak in the Kerr rotation at 0.7 eV originates from Im $\sigma_{xx} = 0$ in combination with a

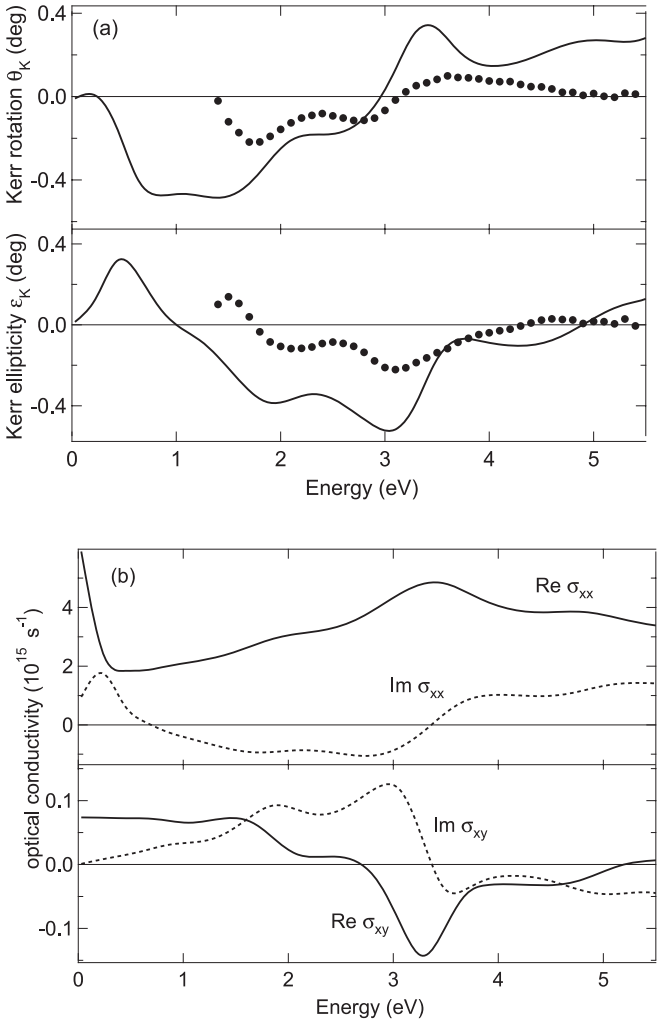


**Figure 2.** Polar Kerr rotation and ellipticity (a) and optical conductivity spectra (b) of AuMnSn versus photon energy. On the left (a), solid lines: calculated; solid circles: measured values [13]. On the right (b), calculated values of the complex diagonal optical conductivity $\sigma_{xx}(\omega)$ and off-diagonal conductivity $\sigma_{xy}(\omega)$.

small Re $\sigma_{xx}$ at the same energy, which leads to a small denominator in equation (1) and hence to an enlarged Kerr rotation.

The off-diagonal element spectrum $\sigma_{xy}(\omega)$ on the other hand has a richer structure and determines the shape of the Kerr rotation and ellipticity spectrum, e.g. the two peaks at 1.85 and 3.1 eV in the ellipticity can be recognized in the computed Im $\sigma_{xy}$ spectrum as well.

The reasons for the described quantitative discrepancies between theory and experiment in the case of AuMnSn are not completely understood yet, since the agreement of the MOKE spectra, calculated within the very same framework, yielded good results in the case of PtMnSb and related half-Heusler compounds [14, 16].

The deviations between the calculated and measured spectra might be partially attributed to the fact that the band structure calculation was performed at nominally 0 K instead of room

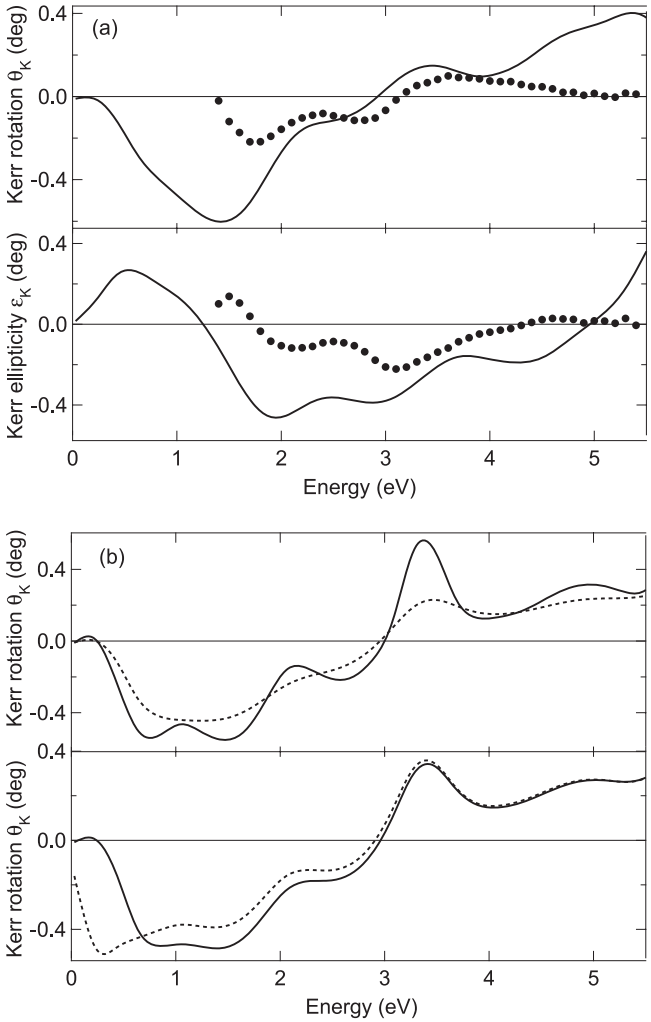


**Figure 3.** On the left (a): polar Kerr rotation and ellipticity of AuMnSn versus photon energy. Solid lines: calculated with artificially reduced magnetic moments ($\mu_{\mathrm{F}}^{\mathrm{Mn}} = 3.65\ \mu_{\mathrm{B}}$). Solid circles: measured values [13]. On the right (b): calculated polar Kerr rotation of AuMnSn versus photon energy. Upper panel: Solid line: relaxation rate $\delta = 0.27$ eV; dashed line: $\delta = 0.54$ eV. Lower panel: with (solid line) and without (dashed line) empirical Drude term.

temperature as used in the experiment. As is well known, the LSDA tends to give lattice constants which are by 2–3% too small [24].

Another effect of non-zero temperature, which should be taken into account, is the reduction of the magnetic moments in the material ($T_{\mathrm{c}} = 600$ K). In order to illustrate this effect for AuMnSn, the magnetic moments were artificially reduced in the ASW calculation and self-consistency was obtained with $\mu_{\mathrm{F}}^{\mathrm{Mn}} = 3.65\ \mu_{\mathrm{B}}$. This value is comparable to the magnetic moment of the Mn at room temperature, cf [11]. The outcome of the subsequent MOKE calculation is shown in figure 3(a). It can be seen at once that the quantitative agreement for $\theta_{\mathrm{K}}$ becomes better in the range 2–4 eV. Although for smaller or higher energies the size of the Kerr rotation remains overestimated. In the case of the Kerr ellipticity, the agreement between theory and experiment does not improve but becomes rather worse, see lower panel

in figure 3(a). Hence a reduction of the magnetic moments cannot be the only reason for the differences in the MOKE spectra. Note that the comparison of figures 2(a) and 3(a) shows that the structures in the calculated $\theta_K$ and $\varepsilon_K$ between 2 and 4 eV are directly linked to the size of the magnetic moment at the Mn sites.

The impact of different relaxation rates $\delta$ and Drude terms on the Kerr rotation spectrum are illustrated in figure 3(b). As one might expect the structures of the spectrum are more pronounced for smaller relaxation rates and vice versa. But even for an almost two times bigger $\delta$ the largest Kerr rotation is still $-0.4°$ at 1.4 eV photon energy. Since most of the structural features are already damped, a further increase of $\delta$ cannot explain the smaller measured Kerr rotation for this photon energy. The lower panel in figure 3(b) compares the Kerr rotation spectrum with and without an empirical Drude term. A decrease of the rotation without an empirical Drude term can be clearly seen between 0.8 and 3 eV. Nonetheless the decrease suffices not to make the quantitative agreement with the measurements much better.

The previous calculations [12] predicted Kerr rotations as large as 0.7° for AuMnSn and 1.2° for AuMnSb, respectively. Apart from the predicted maximal Kerr rotation, the overall shape of the theoretical MOKE spectra also differs from our results. In [12] the same linear-response formalism has been adopted, but the underlying band structure calculations were performed with the full-potential linear muffin-tin orbitals (FP-LMTO) scheme. While we applied here a different computational scheme (ASW), we do not believe that the differences in the MOKE spectra are due to the employed band structure method. Previously, it was shown that the (non-full-potential) ASW and LMTO methods give accurate quantitative agreement for calculated MOKE spectra [16]. Moreover, it has been shown that full-potential linearized augmented plane wave (FP-LAPW) calculations, using the generalized gradient approximation (GGA), lead to practically the same MOKE spectra as the non-full-potential ASW scheme utilizing the LSDA [17]. Thus it appears likely that neither the adopted band structure scheme nor the exchange–correlation functional are responsible for the differences in the computed MOKE spectra.

### *3.3. MOKE of AuMnSb and AuMnIn*

In addition to the already experimentally investigated compound AuMnSn, the MOKE spectra for the two closely related compounds AuMnIn and AuMnSb were calculated. The cause of action and the used input parameters were the same as before. The calculated Kerr rotation and ellipticity are shown in figure 4.

The overall structure of the MOKE spectra of AuMnSb is quite similar to the one of AuMnSn. The largest Kerr rotation in the shown energy range is $-0.84°$ at 0.92 eV and another large rotation occurs at 4 eV. But the shape of the first one is more peak-like and the latter one is broadened compared to AuMnSn. Also in the spectra of the Kerr ellipticities similarities can be recognized: the maximum at a positive angle around 0.5 eV, followed by two minima and another maximum with negative angles. As in the case of the Kerr rotation, the spectra of AuMnSb are stretched towards higher energies.

The trend of changes in the MOKE spectra going from AuMnSb to AuMnSn continues by going further to AuMnIn. Compared to AuMnSn the spectra of AuMnIn are shifted towards higher energies. Both, $\theta_K$ and $\varepsilon_K$, are shifted by approximately 1 eV towards higher energies. The almost vanishing maximum around 0.1 eV of $\theta_K$ of AuMnSn is in the case of AuMnIn shifted towards 0.8 eV and is much more pronounced. The largest Kerr rotation of AuMnIn, 0.64°, can be found at 4.3 eV. In experiments the calculated broad minimum of $-0.34°$ at 2.1 eV might be easier to observe. Similar trends of shifting and broadening of peaks can be seen by comparing the Kerr ellipticity of AuMnIn and AuMnSn, as well.

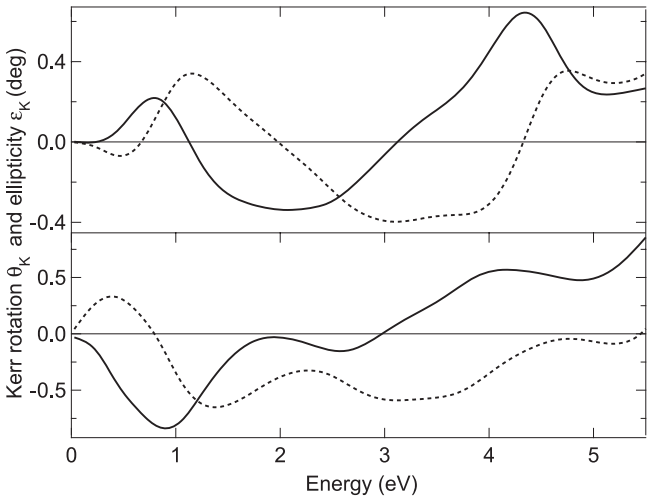


**Figure 4.** Calculated polar Kerr rotation (solid line) and ellipticity (dashed line) for AuMnIn (top) and AuMnSb (bottom), respectively.

## 4. Summary and conclusions

The electronic band structures and the Kerr rotations and ellipticities of the three half-Heusler compounds AuMnX (X = In, Sn, Sb) were calculated with high numerical accuracy. In the case of AuMnSn it was possible to compare our results to the recently published measurements [13]. Although the MOKE spectra could not be reproduced quantitatively, they agree in their overall structure and the overestimation of the MOKE is not as big as in earlier calculations [12]. The reasons for the discrepancies of the calculated Kerr spectra of AuMnSn are not completely understood yet but can be partially explained by temperature effects, leading to a reduction of magnetic moments, as shown. Altogether, the reasonable agreement in the positions of the minima and maxima in the Kerr spectra suggests that the positions of the energy bands are reasonably given by LSDA calculations. The addition of an extra Coulomb '$+U$' term of several electronvolts would considerably shift the energy positions and thus worsen the agreement with experiment.

The close structural relationship of the compounds AuMnIn and AuMnSb to AuMnSn also becomes obvious in the calculated Kerr spectra. Even if there are no MOKE measurements of these compounds available at the moment, we do expect at least an agreement as good as in the case of AuMnSn.

## Acknowledgments

We thank S J Lee for providing us with the experimental results shown in figures 2 and 3. Support through the Swedish Research Council and the Swedish National Infrastructure for Scientific Computing (SNIC) is gratefully acknowledged.

## References

[1] van Engen P G, Buschow K H J, Jongebreur R and Erman M 1983 *Appl. Phys. Lett.* **42** 202
[2] Buschow K H J 1988 *Ferromagnetic Materials* vol 4, ed E P Wohlfarth and K H J Buschow (Amsterdam: Elsevier)

[3] Carey R, Newman D M and Wears M L 2000 *Phys. Rev.* B **62** 1520
[4] de Groot R A, Mueller F M, van Engen P G and Buschow K H J 1983 *Phys. Rev. Lett.* **50** 2024
[5] Pickett W E and Moodera J S 2001 *Phys. Today* **54** 39
[6] Coey J M D, Venkatesan M and Bari M A 2002 *Springer Lecture Notes in Physics* vol 595, ed C Berthier, L P Levy and G Martinez (Heidelberg: Springer)
[7] Kübler J 2000 *Theory of Itinerant Electron Magnetism* (Oxford: Oxford University Press)
[8] Wurmehl S, Fecher G H, Kandpal H C, Ksenofontov V, Felser C, Lin H-J and Morais J 2005 *Phys. Rev.* B **72** 184434
[9] Galanakis I, Mavropoulos Ph and Dederichs P H 2006 *J. Phys.: Appl. Phys.* **39** 765
[10] Neumann A, Offernes L, Kjekshus A and Klewe B 1998 *J. Alloys Compounds* **274** 136
[11] Offernes L, Neumann Torgersen A, Brinks H W, Kjekshus A and Hauback B 1999 *J. Alloys Compounds* **288** 117
[12] Offernes L, Ravindran P and Kjekshus A 2003 *Appl. Phys. Lett.* **82** 2862
[13] Lee S J, Janssen Y, Park J M and Cho B K 2006 *Appl. Phys. Lett.* **88** 121909
[14] Antonov V N, Oppeneer P M, Yaresko A N, Perlov A Ya and Kraft T 1997 *Phys. Rev.* B **56** 13012
[15] Oppeneer P M 2001 *Handbook of Magnetic Materials* vol 13, ed K H J Buschow (Amsterdam: Elsevier)
[16] Oppeneer P M, Antonov V N, Kraft T, Eschrig H, Yaresko A N and Perlov A Ya 1995 *Solid State Commun.* **94** 255
[17] Kuneš J and Novák P 1999 *J. Phys.: Condens. Matter* **11** 6301
[18] Walle C, Offernes L and Kjekshus A 2003 *J. Alloys Compounds* **349** 105
[19] Williams A R, Kübler J and Gelatt C D Jr 1979 *Phys. Rev.* B **19** 6094
[20] Kübler J, Williams A R and Sommers C B 1983 *Phys. Rev.* B **28** 1745
[21] Oppeneer P M, Maurer T, Sticht J and Kübler J 1992 *Phys. Rev.* B **45** 10924
[22] Kubo R 1957 *J. Phys. Soc. Japan* **12** 570
[23] Wang C S and Callaway J 1974 *Phys. Rev.* B **9** 897
[24] Jones R O and Gunnarsson O 1989 *Rev. Mod. Phys.* **61** 689